

Helicopter Fuselage Drag - Combined CFD and Experimental Studies

A. Batrakov, A. Kusyumov, S. Mikhailov, V. Pakhov, A. Sungatullin, M. Valeev, V. Zherekhov and G. Barakos***

**Russia, Kazan, Kazan National Research Technical University, 4240110, Kazan, K. Marx, 10*

***School of Engineering, University of Liverpool, Liverpool, L69 3GH, UK*

Abstract

In this paper, wind tunnel experiments are combined with Computational Fluid Dynamics aiming to analyse the aerodynamics of realistic fuselage configurations. A development model of the ANSAT aircraft and an early model of the AKTAI light helicopter were employed. Both models were tested at the subsonic wind tunnel of KNRTU-KAI for a range of Reynolds numbers, and pitch and yaw angles. The force balance measurements were complemented by PIV investigations for the cases where the experimental force measurements showed substantial unsteadiness. The CFD results were found to be in fair agreement with the test data and revealed some flow separation at the rear of the fuselages. Once confidence on the CFD method was established, further modifications were introduced to the ANSAT-like fuselage model to demonstrate drag reduction via small shape changes.

1. Introduction

The use of Computational Fluid Dynamics (CFD) for the prediction of helicopter aerodynamics is a complex task because of the transient and 3D nature of the flow around the main and tail rotors. Additional complexity arises due to the requirement to model the flow around the fuselage that in many cases behaves as a bluff body with flow separation at its rear part, and around the engine exhausts, fuel tanks, skids etc. The flow separation is partially responsible for an excess amount of drag on such bodies. Further, the inherent flow unsteadiness makes experimentation harder and calls for repeatable sets of measurements to result in data with good confidence intervals. The focus of the present work is the CFD prediction of the helicopter fuselage aerodynamics. This topic, has been the subject of several investigations and a good summary is provided in references [1-3].

A key aspect of the present work is the use of realistic fuselages with the main characteristics encountered in modern designs. For this reason, instead of idealised bodies, early development models of real helicopters were used. In order to have a fuselage representative of modern designs, an approximation to the ANSAT helicopter produced by the JSC Kazan Helicopters (Figure 1) was first considered. A variant of this baseline fuselage, referred to as ANSAT-M2 and shown in Figure 2 was the first model considered. The ANSAT-M2 is one of the many initial designs employed during the development of the ANSAT aircraft, and was used for preliminary aerodynamic studies conducted in the wind tunnel T-1K of KNRTU. The fuselage is not the exact shape of the ANSAT helicopter body with differences concentrated near the engine housing and exhausts. The second case considered in this paper is an early model of the AKTAI light helicopter (Figure 3). It is an asymmetric fuselage shape due to the requirements to house the engine and other equipment. The aerodynamics of several early models of the ANSAT helicopter has also been investigated and these results are presented in references [4-7].

The numerical computations were performed using the in-house CFD tool HMB, developed by Liverpool University. The CFD grids were constructed using the ANSYS ICEM commercial mesh generator. The entire computational domains were resolved using hexahedral grids and the 3D steady Reynolds-Averaged Navier-Stokes (RANS) equations. The computation of the integral and distributed loads on an isolated helicopter fuselage was the first aim of the present investigation.



Figure 1. Photograph of ANSAT helicopter.



Figure 2: Wind tunnel model of the ANSAT-M2 helicopter fuselage.



Figure 3: Wind tunnel model of the AKTAY helicopter fuselage.

2. CFD Mesh Generation

For the CFD grids required around the ANSAT-M2 and AKTAY fuselages the ICEM-Hexa tool has been used. The length of the ANSAT-M2 fuselage was $L_f=1.57$ m, and a reference area of $S_f=0.0694$ m² was used for computing the aerodynamic coefficients of lift and drag. The computational domain was divided in 764 blocks. For the AKTAY wind tunnel model the geometrical parameters were $L_f=1.64$ m, and $S_f=0.1075$ m², while the CFD grid required 1342 blocks. The grid was refined near the fuselage surface (and the resulting y^+ values were near 1) to resolve the laminar sub-layer for better predictions of the friction drag coefficients.

Figure 4 (a) presents a part of the multi-block topology of the grid as well as the surface mesh on the ANSAT-2M fuselage. The surface grid for the AKTAY fuselage is shown in Figure4 (b). A mesh convergence study was first conducted with respect to the number of surface cells and their spatial distribution. For all fuselages, the results presented in this work are nearly mesh independent for the employed Re and turbulence model.

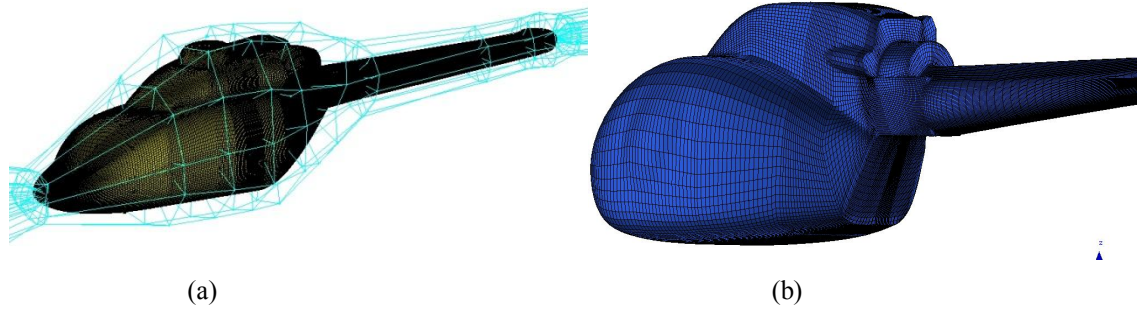


Figure4. (a) Surface mesh and multi-block topology for the ANSAT-2M fuselage.
(b) Surface mesh on the AKTAY model.

3. Prediction of Aerodynamic Force Coefficients

The open test section (of a 2.25m diameter) closed circuit, low speed, wind tunnel T-1K of KNRTU-KAI is equipped with a six-component Prandtl balance. Eight-times measurements were conducted to reduce random experimental errors (system errors, mounting of model, model construction errors, etc) and for plotting error bars around the obtained results.

The standard $k-\omega$ turbulence model was used for computations due to its popularity within the CFD [8-9]. The CFD validation was conducted at Reynolds number of $Re=3.200.000$ and at a free-stream Mach number of $M_\infty=0.1$. These conditions correspond to the experimental investigations. Figure 5 presents the CFD predictions of the lift and drag coefficients for the ANSAT-M2 model in comparison with the wind tunnel experiment data. The error bars shows on the graphs correspond to the experimental confidence intervals. Figure 6 presents the corresponding CD for the AKTAY model. Figures 5, 6 suggest a good agreement between CFD and experimental results for the lift and drag coefficients in the considered range of pitch angles. For all models the drag coefficient values are over predicted in comparison to the experimental data unlike the under-predicted lift coefficient data. The level of agreement with the experiments is satisfactory given the simple RANS model used for computations.

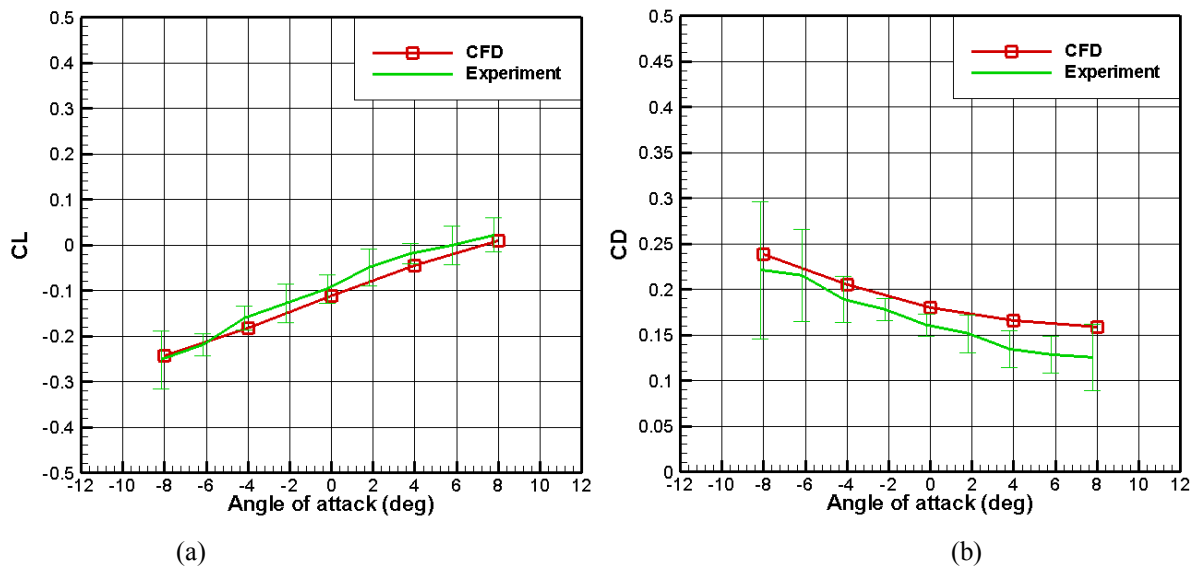


Figure 5. CFD and experimental lift (a) and drag coefficients (b) vs pitch angle for the ANSAT-M2 model.

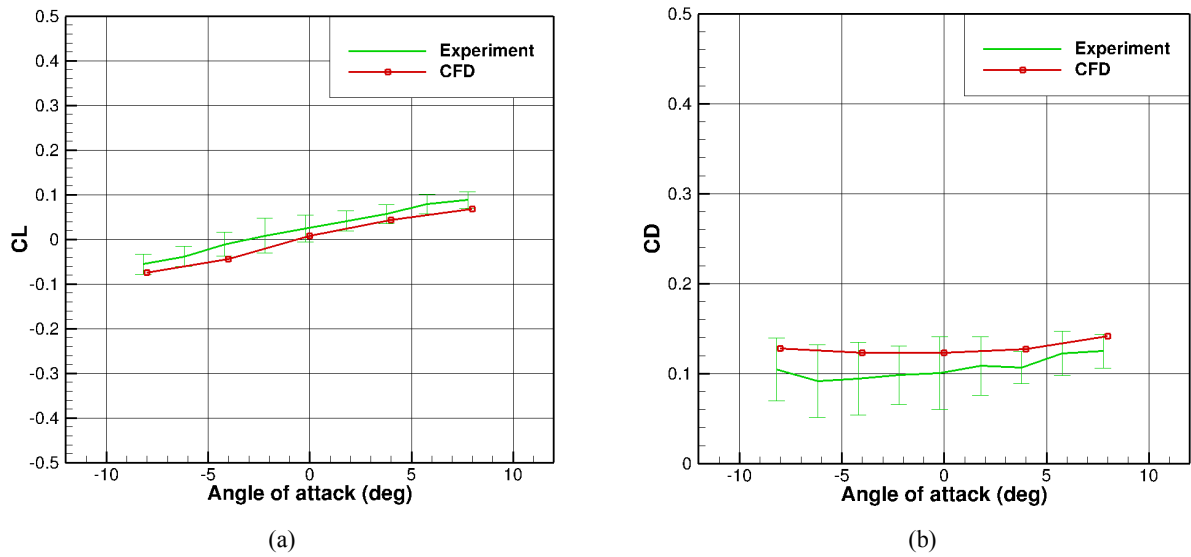


Figure6. CFD and experimental lift (a) and drag (b) coefficients vs pitch angle for the AKTAY model.

4. Distributed Flow Parameters

The integrated loads are complemented by comparisons for distributed flow parameters that allow for a better understanding of the influence of the fuselage geometry on the structure and details. For post-processing of the CFD results the TECPLOT360 commercial visualisation tool was used.

4.1. Experimental and CFD predicted vector fields comparison

Figures 7 and 8 present a comparison of experimental and CFD-predicted vector fields for ANSAT-M2 and AKTAY models. Experimental vector field was obtained using a 2D PIV system.

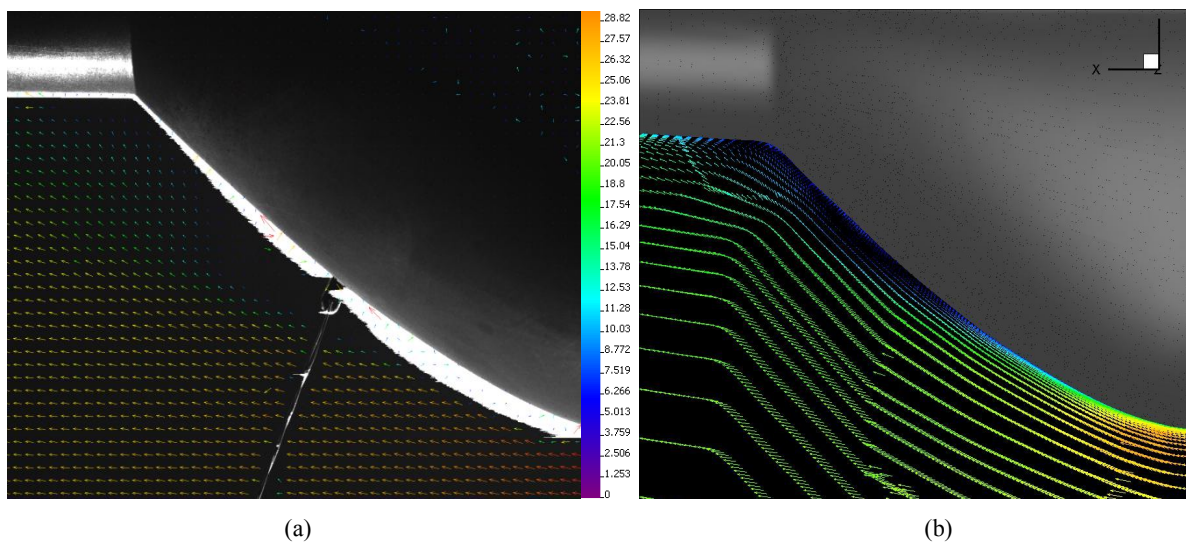


Figure 7. PIV (a) and CFD (b) velocity vector fields at the mid plane of the ANSAT-M2 fuselage for $\alpha=0$ degrees. Comparison around the rear fuselage part is shown.

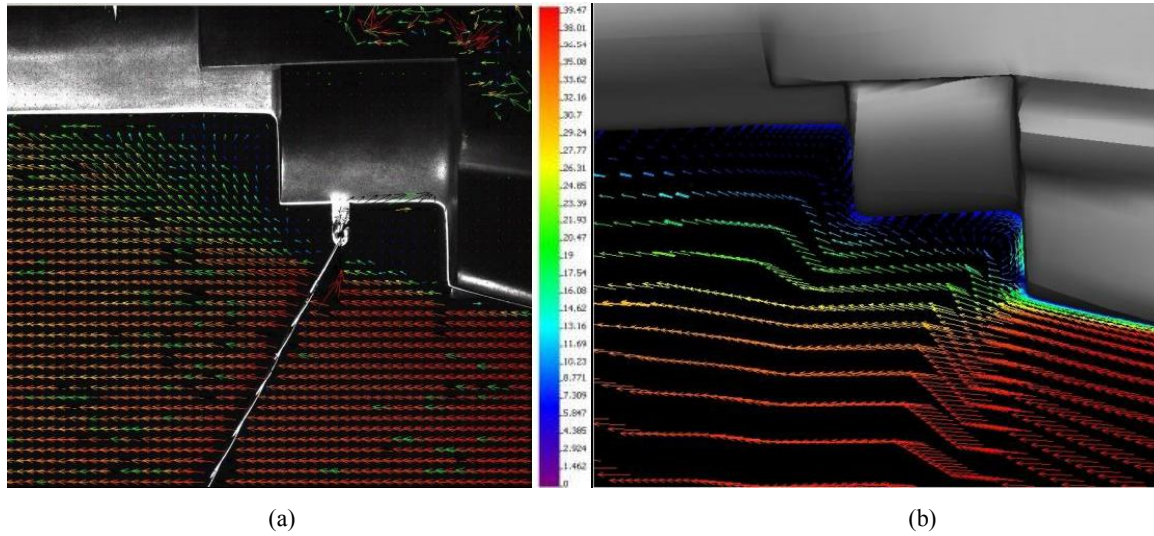
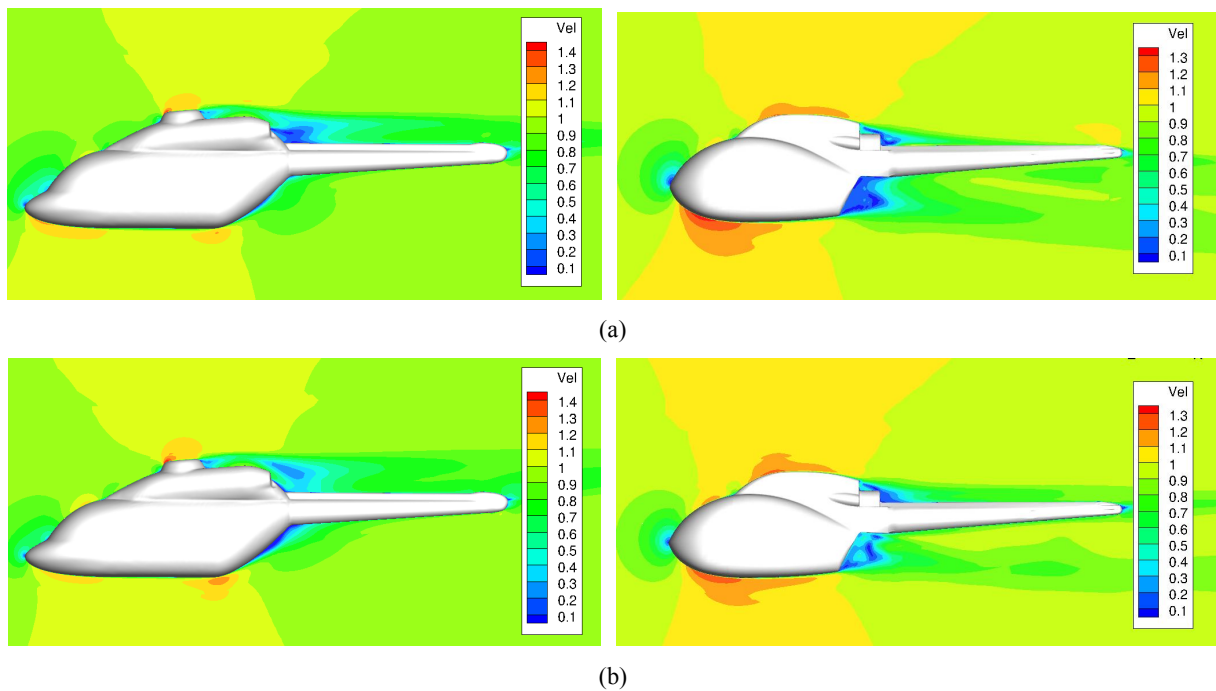


Figure 8. PIV (a) and CFD (b) velocity vector fields at the mid plane of the AKTAY fuselage for $\alpha=0$ degrees. Comparison around the rear fuselage part is shown.

Figures 7 and 8 suggest a good qualitative agreement between CFD and experiments for the considered range of pitch angles. Both CFD and wind tunnel tests revealed a flow separation area although the extend of separation is different between the two models.

4.2 Velocity fields

Figure 9 presents velocity distributions around the mid-plane of the fuselage, and shows the evolution of the separated flow regions with the pitch angle.



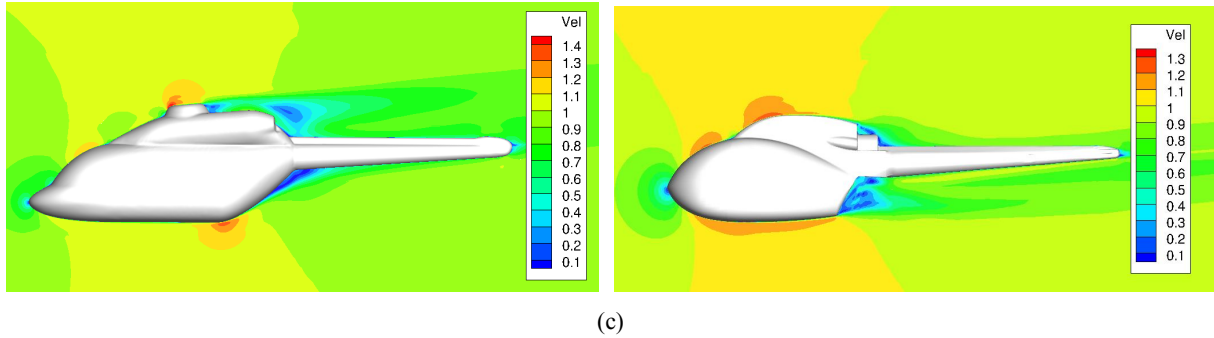


Figure9. CFD prediction of mid-plane velocity for the ANSAT-M2 and AKTAY fuselages at (a) $\alpha=-8$ degrees, (b) 0 degrees, and (c) 8 degrees.

For the ANSAT-M2 model increasing the pitch angle leads to growth of the separation area at rear part of fuselage, but it does not cause the same growth in the drag force (see also Figure 5). Moreover, according to the CFD and experimental data the drag coefficient is monotonically decreasing with the pitch angle. For the AKTAY fuselage the drag coefficient has approximately constant values within the considered range of attack angles. Figure 10 presents the velocity fields at a horizontal plane under the tail boom of the ANSAT-M2 and AKTAY fuselages.

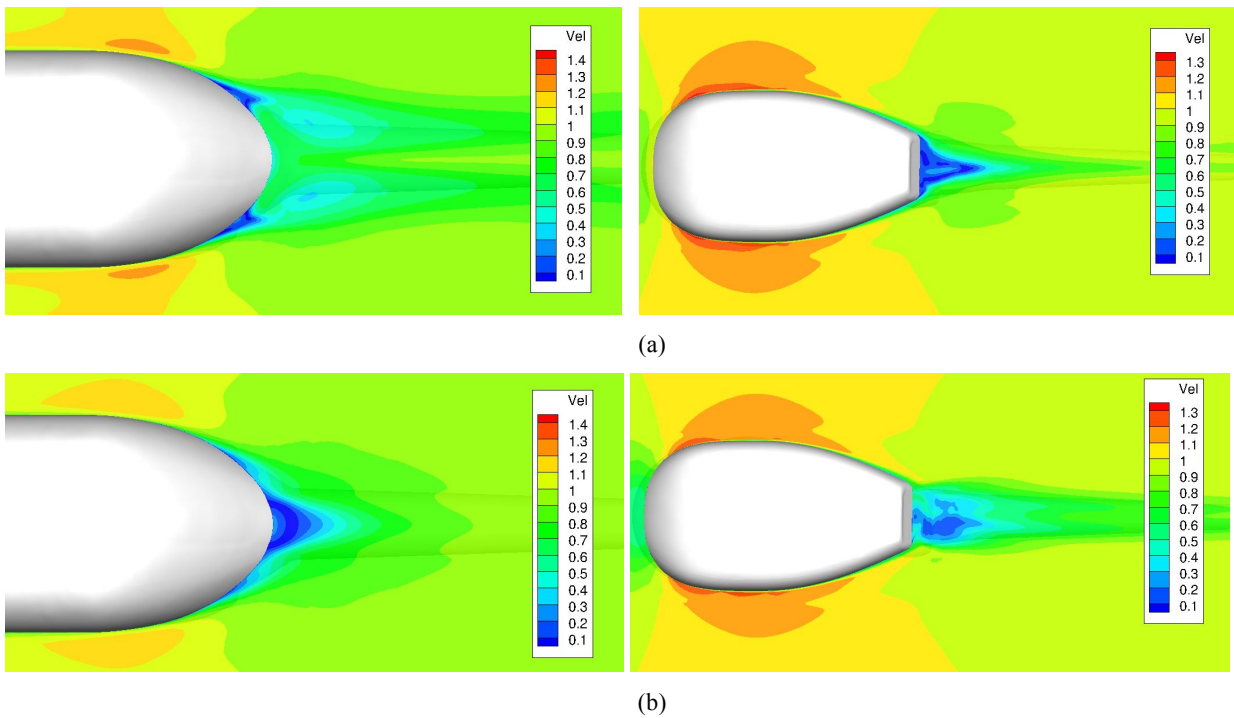


Figure 10. CFD prediction of horizontal plane velocity for the ANSAT-M2 and AKTAY fuselages at $\alpha=-8$ degrees (a) and 8 (b) degrees

At $\alpha=8$ degrees a separation area centred in the considered section is located at the symmetry plane of ANSAT-M2 fuselage (Figure 10b). For $\alpha=-8$ degrees Figure 10 (a) reveals the presence of two separation cores at the horizontal plane. The ANSAT-M2 geometry is more streamlined in comparison to the AKTAY model. For the AKTAY model the topology of separation area is the same for $\alpha=-8$ degrees and for $\alpha=8$ degrees. For this reason the drag coefficient value for $\alpha=-8$ degrees is close to the drag coefficient for $\alpha=8$ degrees. This behaviour was expected for a body shaped like the AKTAY that has separated flow always present.

4.3. Further flow visualisation

Iso-surfaces corresponding to value velocity magnitude of $V=0.2V_\infty$ are used for visualisation, where V_∞ is free stream velocity. For areas without flow separation the iso-surfaces of $V=\text{constant}$, are close to the fuselage surface and the geometry of the iso-surfaces corresponds to fuselage geometry. In the separation zones, the iso-surfaces detach from the fuselage surface and this allows the visualisation of the zones. Figure 11 presents iso-surfaces for different pitch angles.

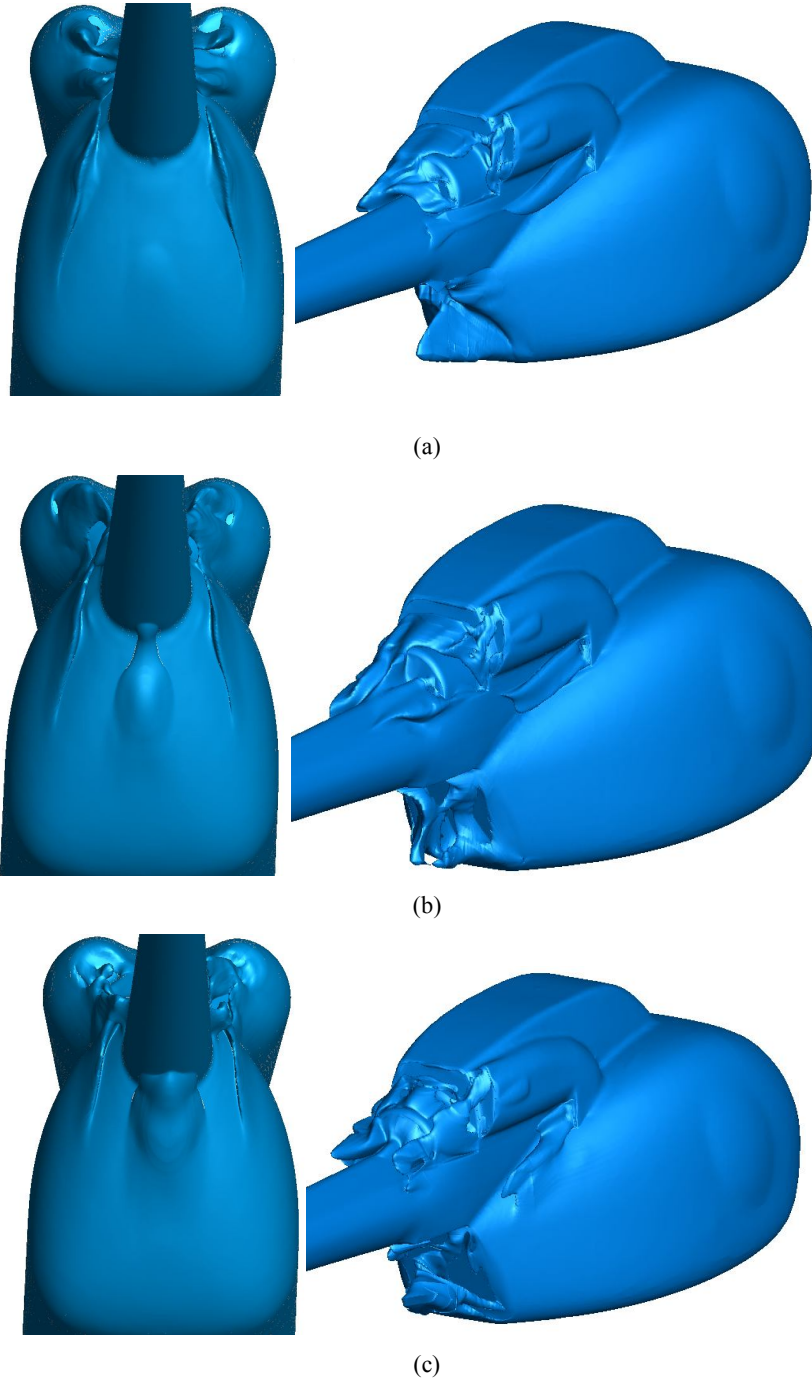


Figure 11. Iso-surfaces corresponding to $V=0.2V_\infty$ for the ANSAT-M2 and the AKTAY fuselages
(a) $\alpha=-8$ degrees, (b) $\alpha=0$ degrees, and (c) $\alpha=8$ degrees.

Figure 11 shows the different character of the separation areas for the streamlined (ANSAT-M2) and the bluff (AKTAY) fuselages. In general, the shape of the iso-surfaces corresponds to the flow fields presented in Figure 10.

For the ANSAT-M2 model there are two areas of separation with different character of development with respect to the pitch angle. Both areas of separation are located symmetrically to the fuselage mid-plane. This separation region is maximised for negative pitch angles and it maintains the same structure with two contra-rotating vortices. The intensity (geometrical size) of the separation is maximal for a negative pitch angle of -8 degrees and monotonically decreases with respect to the pitch angle. A different separated flow region with a single core of separation is located at the place of fuselage, near the tail boom junction. The intensity of this separated flow region is maximal for a positive pitch angle of 8 degrees. At a pitch of -8 degrees, this separation region almost disappears. The flow structure for the AKTAY model is different because of the blunt rear fuselage. For the AKTAY model the flow at the rear part of fuselage has a more unsteady character and is less sensitive to the pitch angle.

4.4. Flow stream lines

Figure 12 shows stream lines in the ZY plane that is normal to the free-stream velocity vector. For the ANSAT-M2 model, the location of vortexes at the rear part of fuselage corresponds to two cores of separation present at -8 degrees. At zero and 8 degrees of pitch the flow is more attached. The flow structure at the rear part of AKTAY fuselage appears to be separated regardless of the pitch angle and the size of the separated flow region is independent of the pitch angle.

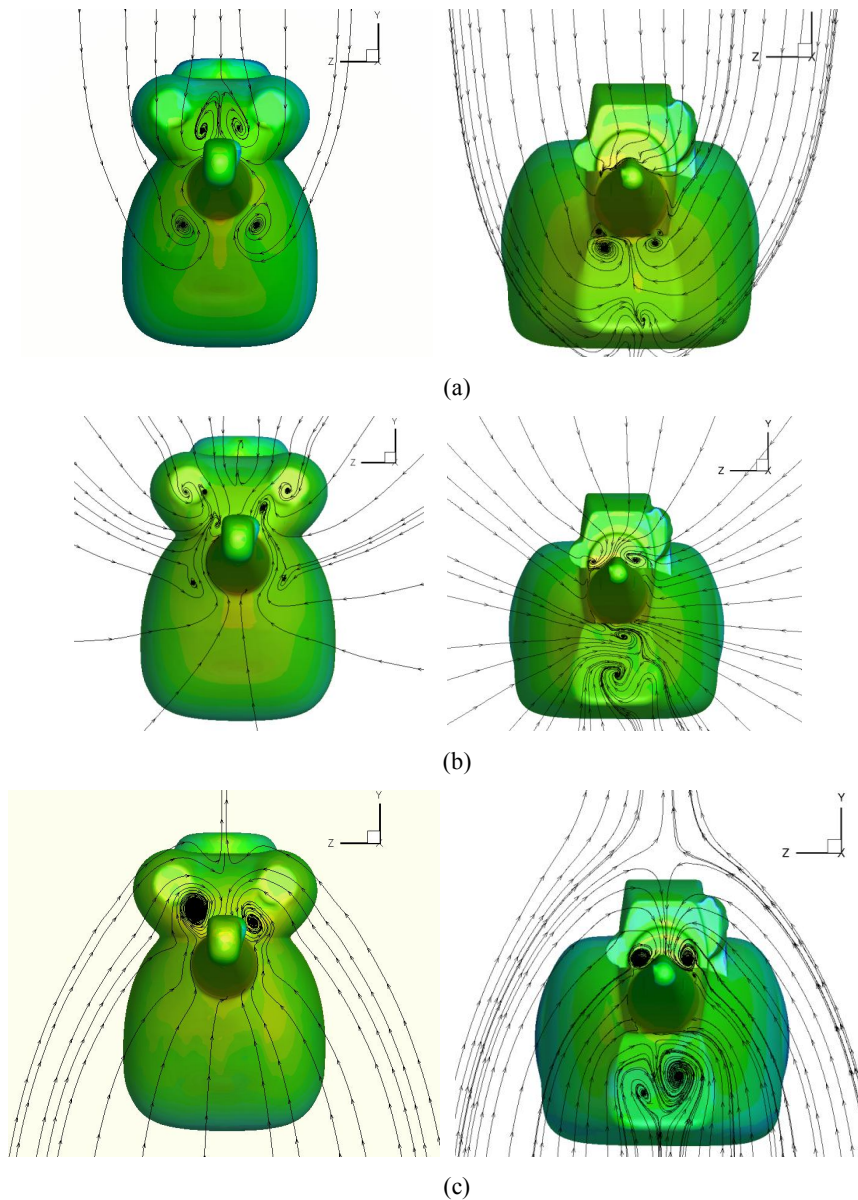


Figure 12. Stream functions for ANSAT-M2 and AKTAY fuselages
(a) $\alpha=-8$ degrees, (b) 0 degrees, and (c) 8 degrees.

5. Conclusion and Future work

The flow around the simplified ANSAT and AKTAY helicopter fuselages was analysed. The experimental values of drag and lift coefficients were compared with CFD data with good agreement. The structure of the separated flow region at the rear of both fuselages was also analysed at different pitch angles. It is shown that for the streamlined shape of the ANSAT-M2 model, the flow at rear part of fuselage has two main separation regions. This is not the case for the AKTAY where the flow separation covers a single large area and is present, regardless of the pitch angle. In the future, the effect of the helicopter rotor on the fuselage drag will be considered along with further investigations in the best way to design the rear fuselage for drag reduction.

Acknowledgments

This work is supported by the “Leading Scientist” grant of the Russian Federation, under order 220 of the Russian Ministry of Education. The authors would like to acknowledge the Kazan Helicopter Plant for providing the initial fuselage shapes for this research.

References

- [1] Alascio A. D', Pahlke K. and Chuiton F. Le. 2004. Application of a Structured and an Unstructured CFD method to the Fuselage Aerodynamics of the EC145 Helicopter, Prediction of the Time Averaged Influence of the Main Rotor. In: *ECCOMAS European Congress on Computational Methods in Applied Sciences and Engineering*.
- [2] Chuiton F. Le, D'Alascio A., Barakos G.N., Steijl R., Schwamborn D. and Ludeke H. 2009. EC145 Helicopter Fuselage - An Industrial Case. In: *DESider - A European Effort on Hybrid RANS-LES Modelling*, W. Haase, M. Braza, A. Revell (Eds.), *Notes on Numerical Fluid Mechanics and Multidisciplinary Design*. Vol. 103, pp. 250-260, Springer Verlag.
- [3] Bridgeman J. O. and Lancaster G. T. 2010. Predicting Hub Drag on Realistic Geometries. *Presented at the American Helicopter Society Aeromechanics Specialists' Conference, Holiday Inn Fisherman's Wharf, San Francisco, California, USA*.
- [4] Kusyumov A.N., Mikhailov S.A., Nikolaev E.I., Shilova N.A., Garipov A.O. 2011. Simulation of Flow around the Fuselage of “ANSAT” Helicopter. *ASME 2011 International Mechanical Engineering Congress & Exposition IMECE2011*, Denver, Colorado, USA.
- [5] Pahov V., Valiev M., Zherekhov V., Makarova L., Kusyymov A. and George Barakos. 2012. Creating a Database for Validation of Predictive Methods for Rotorcraft. *47th International Symposium of Applied Aerodynamics*, Paris, France.
- [6] Kusyumov A.N., Mikhailov S.A., Romanova E.V., Garipov A.O., Nikolaev E.I., Barakos G. 2012. Simulation of Flow around Isolated Helicopter Fuselage. *EFM 2012 conference*, Hradec Kralove, Czech Republic.
- [7] Kusyumov A., Mikhailov S., Garipov A., Nikolaev E., Barakos G. 2012. CFD Simulation of Fuselage Aerodynamics of the “ANSAT” Helicopter Prototype. *Transactions on Control and Mechanical Systems*, Vol. 1, No 7, pp. 318 – 324.
- [8] Lienard C., Le Pape A. and Verbeke C. 2012. Numerical and Experimental Investigation of Helicopter Fuselage Drag Reduction Using Active Flow Control. *American Helicopter Society 68th Annual Forum*, Fort Worth, Texas, USA.
- [9] Dietz M., Kneisch T., Roth G., D'Alascio A. and Schimke D. 2012. EC145 T2: Comprehensive and Challenging Industrial CFD Applications. *American Helicopter Society 68th Annual Forum*, Fort Worth, Texas, USA.